

Bose-Einstein condensates in 1D optical lattices: nonlinearity and Wannier-Stark spectra

Ennio Arimondo, Donatella Ciampini and Oliver Morsch
*CNR-INFM and CNISM, Dipartimento di Fisica E.Fermi,
Università di Pisa, Via Buonarroti 2, I-56127 Pisa, Italy*

We present our experimental investigations on the subject of nonlinearity-modified Bloch-oscillations and of nonlinear Landau-Zener tunneling between two energy bands in a rubidium Bose Einstein condensate in an accelerated periodic potential. Nonlinearity introduces an asymmetry in Landau-Zener tunneling. We also present measurements of resonantly enhanced tunneling between the Wannier-Stark energy levels for Bose-Einstein condensates loaded into an optical lattice.

PACS numbers:

I. INTRODUCTION

The development of powerful laser cooling and trapping techniques has made possible the controlled realization of dense and cold gaseous samples, thus opening the way for investigations in the ultracold temperature regimes not accessible with conventional techniques. A Bose-Einstein condensate (BEC) represents a peculiar gaseous state where all the particles reside in the same quantum mechanical state. Therefore BEC's exhibit quantum mechanical phenomena on a macroscopic scale with a single quantum mechanical wavefunction describing the external degrees of freedoms. That control of the external degrees of freedom is combined with a precise control of the internal degrees. The BEC investigation has become a very active area of research in contemporary physics. The BEC study encompasses different subfields of physics, i.e., atomic and molecular physics, quantum optics, laser spectroscopy, solid state physics. Atomic physics and laser spectroscopy provide the methods for creating and manipulating the atomic and molecular BECs. However owing to the interactions between the particles composing the condensate and to the configuration of the external potential, concepts and methods from solid state physics are extensively used for BEC description.

Quantum mechanical BEC's within the periodic potential created by interfering laser waves ("optical lattices") have attracted a strongly increasing interest[1, 2, 3, 4]. In particular, the formal similarity between the wavefunction of a BEC inside the periodic potential of an optical lattice and electrons in a crystal lattice has triggered theoretical and experimental efforts alike. BEC's inside optical lattices share many features with electrons in solids, but also with light waves in nonlinear materials and other nonlinear systems. However, the experimental control over the parameters of BEC and of the periodic potential make it possible to enter regimes inaccessible in other systems. Many phenomena from condensed matter physics, such as Bloch oscillations and Landau-Zener tunneling have since been shown to be observable also in optical lattices. BEC in an optical lattice even made possible the observation of a quantum phase transition that had, up to then, only been theoretically predicted for condensed matter systems [5]. However an important difference between electrons in a crystal lattice and a BEC inside the periodic potential of an optical lattice is the strength of the self interaction between the BEC components and hence the magnitude of the nonlinearity of the system. Electrons are almost noninteracting whereas atoms inside a BEC interact strongly. A perturbation approach is appropriate in the former case while in the latter the full nonlinearity must be taken into account. Generally, atom-atom interactions in Bose-Einstein condensates lead to rich and interesting nonlinear effects. Most experiments to date have been carried out in the regime of shallow lattice depth, for which the system is well described by the Gross-Pitaevskii equation, a mean-field equation. Moreover, the nonlinearity induced by the mean-field of the condensate has been shown both theoretically and experimentally to give rise to instabilities in certain regions of the Brillouin zone. These instabilities are not present in the corresponding linear system, i.e. the electron system.

The present text initially describes the construction of the optical lattice periodic potential for cold atoms in Sec. II. The following Section reports the analysis of the condensate interference pattern when released from the optical lattice. In Sec. IV the nonlinear term within the Gross-Pitaevskii equation describing the dynamics of a Bose-Einstein condensation is introduced. The following Sections report experimental results on the Bloch oscillations, on the nonlinear Landau-Zener quantum tunneling and on the resonantly enhanced quantum tunneling. A short conclusion terminates the presentation.

II. OPTICAL LATTICE

In order to trap a Bose-Einstein condensate in a periodic potential, it is sufficient to exploit the interference pattern created by two or more overlapping laser beams and the light force exerted on the condensate atoms. Optical lattices work on the principle of the ac Stark shift. When an atom is placed in a light field, the oscillating electric field of the latter induces an electric dipole moment in the atom. The interaction between this induced dipole and the electric field leads to an energy shift ΔE of an atomic energy level. When we take two identical laser beams and make them counterpropagate in such a way that their cross sections overlap completely see Fig. 1(a), we expect the two beams to create an interference pattern, with a distance $d_L = \lambda/2$ between two neighboring maxima or minima of the resulting light intensity. The potential seen by the atoms is then

$$V(x) = V_0 \cos^2\left(\frac{\pi x}{d}\right) = \frac{V_0}{2} \left[1 + \cos\left(\frac{2\pi x}{d_L}\right)\right], \quad (1)$$

where the lattice depth V_0 is determined by the light shifts ΔE produced by the individual laser beams. The easiest option to create a one-dimensional optical lattice is to take a linearly polarized laser beam and retro-reflect it with a high-quality mirror. If the retro-reflected beam is replaced by a second phase-coherent laser beam as obtained, for instance, by dividing a laser beam in two, another degree of freedom is introduced. It is now possible to have a frequency shift $\Delta\nu_L$ between the two lattice beams. The periodic lattice potential will now no longer be stationary in space but move at a velocity $v_{\text{lat}} = d_L \Delta\nu_L$. If the frequency difference is varied at a rate $\partial\Delta\nu_L/\partial t$, the lattice potential will be accelerated with $a_{\text{lat}} = d_L \partial\Delta\nu_L/\partial t$. Clearly, in the rest frame of the lattice there will be a force

$$F = -M a_{\text{lat}} = -M d_L \frac{\partial\Delta\nu_L}{\partial t} \quad (2)$$

acting on the condensate atoms. This gives us a powerful tool for manipulating a BEC inside an optical lattice.

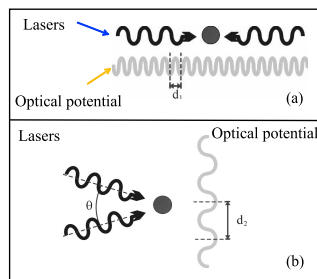


FIG. 1: Representation of the laser configuration creating an optical lattice in the counterpropagating geometry, in (a), and in the angle tuned geometry, in (b)

Another degree of freedom of a 1D lattice realized with two laser beams is the lattice constant. The spacing d_L between two adjacent wells of a lattice resulting from two counterpropagating beams can be enhanced by making the beams intersect at an angle $\theta \neq \pi$, see Fig. 1(b). This will give rise to a periodic potential with lattice constant

$$d_L = \frac{\lambda}{2 \sin(\theta/2)}. \quad (3)$$

To simplify the notation, in the following we shall always denote the lattice constant by d_L and all the quantities derived from it, regardless of the lattice geometry that was used to achieve it. In particular the recoil energy E_R and the recoil frequency ν_R of an atom with mass M are

$$E_R = \hbar \nu_R = \frac{\hbar^2 \pi^2}{2M d_L^2}, \quad (4)$$

and the recoil velocity $v_R = \hbar\pi/(d_L M)$. Naturally, by adding more laser beams one can easily create two- or three-dimensional lattices[4].

The description of the propagation of noninteracting matter waves in periodic potentials is straightforward once one has found the eigenstates and corresponding eigenenergies of the system. The eigenstates are found in by applying Bloch's theorem, which states that the eigenfunctions have the form [6]

$$\phi_{n,q}(x) = e^{iqx} u_{n,q}(x), \quad (5)$$

where $\hbar q$ is referred to as quasimomentum and n indicates the band index, the meaning of which will become clear in the following discussion. The quasimomentum q appearing in the Bloch's theorem can always be confined to the first Brillouin zone $(-q_R, q_R)$ with $q_R = \pi/d_L$, because any q' not in the first Brillouin zone can be written as $q' = q + G$, where G is a reciprocal lattice vector and q does lie in the first zone. The eigenenergies $E^n(q)$ of the above eigenstates depend on the potential depth $V_0 = sE_R$ and, additionally, on the quasimomentum q . In Fig. 2, we summarize the properties of the eigenbasis for a shallow potential $V_0 = 2E_R$. The eigenenergies form bands that are separated by a gap in the energy spectrum, i.e., certain energies are not allowed. Since the gap energy E_{gap}^n between the n th and $(n+1)$ th band scales with V_0^{n+1} in the weak potential limit, it only has appreciable magnitude between the lowest and first excited band. A particle with high energy is very well described as a free particle and the influence of the periodic potential is negligible in this case. It is important to note that for energies near the Brillouin zone edge of the lowest band, the eigenstate probability distribution is a periodic $\sqrt{2} \sin \frac{2\pi x}{2d_L} e^{i\frac{\pi x}{2d}}$ function, its maxima coinciding with the potential minima and the phase changing by π between adjacent wells. This is the well-known sinusoidal Bloch state at the Brillouin zone edge, in the literature also referred to as a staggered mode. In the limit of deep periodic potentials, also referred to as the tight-binding limit, the eigenenergies of the low lying bands are only weakly dependent on the quasimomentum.

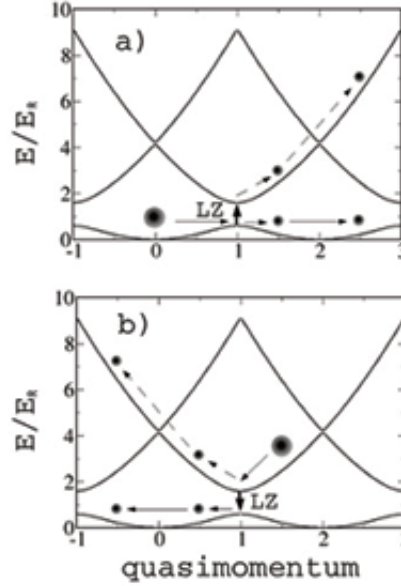


FIG. 2: Band structure of a BEC in an optical lattice ($V_0 = 2E_R$) and LZ-tunneling (ground to excited state (a) and excited to ground state (b)). When the BEC is accelerated across the edge of the Brillouin zone (BZ) at quasimomentum $q/q_R = 1$, LZ tunneling occurs. After the first crossing of the edge of the Brillouin zone increasing the lattice depth and decreasing the acceleration leads to a much reduced tunneling rate from the ground state band at successive BZ-edge crossings, as shown in (a) for the ground to excited state tunneling and in (b) for excited to ground state

The wave-packet dynamics of a particle in a periodic potential in the presence of an additional external potential, i.e., with an external force, is generally not easy to solve. The problem becomes relatively simple, though, as soon as the width of the wave packet in quasimomentum space is small and thus the wave packet can be characterized by a single mean quasimomentum $q(t)$ at time t . An external force then leads to a time-dependent $q(t)$ via

$$\hbar \dot{q}(t) = F. \quad (6)$$

In the case of a constant force F e.g., due to the gravitational field, this results in

$$q(t) = q(t=0) + \frac{Ft}{M}. \quad (7)$$

In addition, the velocity $v_n(q)$ of the particle in the n band is given by the group velocity of the underlying wavepacket

$$v_n(q) = \frac{1}{\hbar} \frac{\partial E_n(q)}{\partial q}. \quad (8)$$

The above equations determine that the rate of change of the quasimomentum is given by the external force, but the rate of change of the wavepacket's momentum is given by the total force including the influence of the periodic field of the lattice. In the case of a constant force, the velocity at time t is

$$v_n(q(t)) = v_n(q(t=0)) + \frac{Ft}{M}. \quad (9)$$

Since v_n is periodic in the reciprocal lattice, the velocity is a bounded and oscillatory function of time. Therefore the result of the force is not an acceleration of the wave packet, and instead the wavepacket will show an oscillatory behavior in real space. The velocity oscillatory motion is known as Bloch oscillations [7] and the period as the Bloch time

$$T_B = \frac{2\pi\hbar}{Fd_L} = \frac{1}{F_0\nu_R}, \quad (10)$$

where we have introduced a dimensionless force $F_0 = Fd_L/E_R$.

In the case of a strong external force acting on matter waves in periodic potentials, transitions into higher bands can occur as schematically represented in Fig. 2. In the context of electrons in solids, this is known as the Landau-Zener (LZ) breakdown [8, 9], occurring if the applied electric field is strong enough for the acceleration of the electrons to overcome the gap energy separating the valence and conduction bands. It was shown in [9] that for a given acceleration a_L corresponding to a constant force, one can deduce a tunneling probability across the first-second band gap in the adiabatic limit

$$P_{LZ} = e^{-\frac{\pi^2 V_0^2}{32 F_0}}. \quad (11)$$

The resulting wavepacket dynamics is shown in Fig. 2, where LZ tunneling, from $n = 1$ to $n = 2$ band, leads to a splitting of the wave function.

III. ANALYSIS OF THE INTERFERENCE PATTERN

Doing experiments with condensates in optical lattices is useful only if one is able to extract information from the system once the experiment has been carried out. There are essentially two methods for retrieving information from the condensate: in situ and after a time of flight. In the former case, one can obtain information about the spatial density distribution of the condensate, its shape, and any irregularities on it that may have developed during the interaction with the lattice. Also, the position of the center of mass of the condensate can be determined. Looking at a condensate released from a lattice after a time of flight, typically on the order of a few milliseconds, amounts to observing its momentum distribution. When the atomic system is in a steady state, the condensate is distributed among the lattice wells (in the limit of a sufficiently deep lattice in order for individual lattice sites to have well-localized wavepackets). If the lattice is now switched off suddenly, the individual (approximately) Gaussian wavepackets at each lattice site will expand freely and interfere with one another. The resulting spatial interference pattern after a time-of-flight of t will be a series of regularly spaced peaks with spacing $2v_R t$, corresponding to the various diffraction orders. In the case of a condensate that is very elongated along the lattice direction, to a good approximation we initially have an array of equally spaced Gaussians of a width d determined by the lattice depth. Figure 3 shows a typical time-of-flight interference pattern of a condensate released from an optical lattice (plus harmonic trap) for a lattice depth $V_0 = 10E_R$. From the spacing of the interference peaks and the time of flight, one can immediately infer the recoil momentum of the lattice and hence the lattice constant d . Furthermore, from the relative height of the side peaks corresponding to the momentum classes $\pm 2\pi/d_L$, one can calculate the lattice depth. The top interference pattern was produced by a condensate at rest with zero quasimomentum. Instead the bottom interference pattern was produced by a condensate with quasimomentum at the edge of the Brillouin zone, in the staggered state with the condensate wavefunction changing by π between adjacent wells.

IV. NONLINEAR OPTICAL LATTICE

The motion of a Bose-Einstein condensate in a 1D optical lattice experiencing an acceleration a_L is described by the Gross-Pitaevskii equation

$$i\hbar \frac{\partial \psi}{\partial t} = \frac{1}{2M} \left(-i\hbar \frac{\partial}{\partial x} + Ma_L t \right)^2 \psi + \frac{V_0}{2} \cos\left(\frac{\pi x}{d_L}\right) \psi + \frac{4\pi\hbar^2 a_s}{M} |\psi|^2 \psi. \quad (12)$$

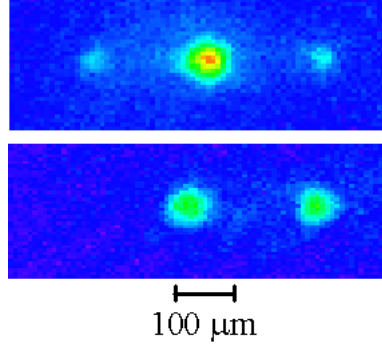


FIG. 3: Interference pattern of a Bose-Einstein condensate released from a one-dimensional optical lattice of depth $V_0 = 10E_R$ after a time of flight of 20 ms. In the top pattern the lattice was at rest, whereas in the bottom one the condensate had been accelerated to v_R , i.e., its quasimomentum was at the edge of the Brillouin zone

The s -wave scattering length a_s determines the nonlinearity of the system. Equation 12 is written in the comoving frame of the lattice, so the inertial force $-Ma_L$ appears as a momentum modification. The wavefunction ψ is normalized to the total number of atoms in the condensate and we define n_0 as the average uniform atomic density. Defining the dimensionless quantities $\tilde{x} = 2\pi x/d_L$, $\tilde{t} = 8E_R t/\hbar$, and rewriting $\tilde{\psi} = \psi/\sqrt{n_0}$, $\tilde{v} = V_0/16E_R$, $\tilde{\alpha} = Ma_L d_L/16E_R \pi$, $C = a_s n_0 d_L^2/\pi$, 12 is cast in the following form:

$$i\frac{\partial\psi}{\partial t} = \frac{1}{2}\left(-i\frac{\partial}{\partial x} + \alpha t\right)^2 \psi + v \cos(x)\psi + C|\psi|^2\psi, \quad (13)$$

where we have replaced \tilde{x} with x , etc. In the neighborhood of the Brillouin zone edge we can approximate the wavefunction by a superposition of two plane waves, assuming that only the ground state and the first excited state are populated. We then substitute in 13 a normalized wavefunction

$$\psi(x, t) = a(t)e^{iqx} + b(t)e^{i(q-1)x}. \quad (14)$$

Projecting on this basis, linearizing the kinetic terms and dropping the irrelevant constant energy, 13 assumes the form

$$i\frac{\partial}{\partial t} \begin{pmatrix} a \\ b \end{pmatrix} = \left[-\frac{\alpha t}{2}\sigma_3 + \frac{v}{2}\sigma_1\right] \begin{pmatrix} a \\ b \end{pmatrix} + \frac{C}{2}(|b|^2 - |a|^2)\sigma_3 \begin{pmatrix} a \\ b \end{pmatrix}, \quad (15)$$

where σ_i $i = 1, 2, 3$ are the Pauli matrices. The adiabatic energies of 15 have a butterfly structure at the band edge of the Brillouin zone for $C \geq v$ [10], but in the present work we only consider a regime where $C \ll v$, hence that structure plays no role.

In the linear regime ($C = 0$), evaluating the transition probability in the adiabatic approximation, we find the linear LZ formula for the tunneling probability P_{LZ} given by 11. Therefore for $C = 0$ the tunneling probability is the same for both tunneling directions whereas for $C \neq 0$ the two rates are different. In the nonlinear regime, as the nonlinear parameter C grows, the lower to upper tunneling probability grows as well until an adiabaticity breakdown occurs at $C = v$ [10]. The upper to lower tunneling probability, on the other hand, decreases with increasing nonlinearity.

The asymmetry in the tunneling transition probabilities can be explained qualitatively as follows: The nonlinear term of the Schrödinger equation acts as a perturbation whose strength is proportional to the energy level occupation. If the initial state of the condensate in the lattice corresponds to a filled lower level of the state model, then the lower level is shifted upward in energy while the upper level is left unaffected. This reduces the energy gap between the lower and upper level and enhances the tunneling. On the contrary, if all atoms fill the upper level then the energy of the upper level is increased while the lower level remains unaffected. This enhances the energy gap and reduces the tunneling. The overall balance leads to an asymmetry between the two tunneling processes.

The nonlinear regime may be reinterpreted by writing 15 as

$$i\frac{\partial}{\partial t} \begin{pmatrix} a \\ b \end{pmatrix} = \left[-\frac{\alpha t}{2}\sigma_3 + \frac{v}{2}\sigma_1\right] \begin{pmatrix} a \\ b \end{pmatrix} - \frac{C}{2} \begin{pmatrix} |a|^2 & -b^*a \\ -a^*b & |b|^2 \end{pmatrix} \begin{pmatrix} a \\ b \end{pmatrix}. \quad (16)$$

The nonlinear off-diagonal terms modify the interaction term v in a way equivalent to a Rabi frequency in the two-level model. In 16 we identify an offdiagonal term $v + C a^*b$ which acts as an effective potential. Thus for small C values

we can modify the linear LZ formula 11 to include nonlinear corrections, substituting the potential $v = V_0/16E_R$ with the effective potential $v_{\text{eff}} = V_{\text{eff}}/16E_R \equiv |v + C a^* b|$ (modulus is needed since $a^* b$ is complex). The expression for v_{eff} is

$$v_{\text{eff}} = v \sqrt{1 \pm \frac{C}{v} + \frac{C^2}{4v^2}}, \quad (17)$$

where the upper and lower signs corresponds to initial conditions of excited/ground states.

V. BLOCH OSCILLATIONS

A fundamental property of a quasiparticle in a periodic potential subject to an external static force is its localization by Bragg reflections at the boundary of the Brillouin zone, which leads to temporal and spatial oscillations known as Bloch oscillations [7]. Related fundamental transport phenomena are the nonresonant LZ tunneling into a continuum of states of another Bloch band and the resonant LZ tunneling between anticrossing Wannier-Stark states of neighboring Bloch bands. Bloch oscillations were first observed as time-resolved oscillations of wave packets of photo-excited "hot" electrons in biased semiconductor superlattices. Later Bloch oscillations and LZ tunneling were observed in ensembles of cold atoms [11, 12, 13]. During the last decade, there were experimentally realized time-resolved Bloch oscillations of coherent electron wave packets in semiconductor superlattices [14, 15] subjected to combined electric and magnetic fields. The progress in the fabrication and investigation of complex optical nanostructures has allowed for direct experimental observations of one-dimensional optical Bloch oscillations of an optical laser field in dielectric structures with a transversely superimposed linear ramp of the refractive index [16, 17]. A periodic distribution of the refractive index plays a role of the crystalline potential, and the index gradient acts similarly to an external force in a quantum system. This force causes the laser beam to move across the structure while experiencing Bragg reflections on the high-index and total internal reflection on the low-index side of the structure, resulting in an optical analogue of Bloch oscillations. Bloch oscillations and LZ tunneling from the first to second energy band was also demonstrated experimentally in two-dimensional photonic structures [18]. Most recently, acoustic Bloch oscillations and resonant LZ tunneling of phononic wave packets were observed in perturbed ultrasonic superlattices [19].

We report here results for Bloch oscillations in experiments with Bose-Einstein condensates adiabatically loaded into one-dimensional optical lattices. In particular, we discuss the dynamics of the BEC when the periodic potential provided by the optical lattice is accelerated, leading to Bloch oscillations [20, 21]. The condensate was loaded adiabatically into the (horizontal) optical lattice with lattice constant $d_L = 390$ nm immediately after switching off the magnetic trap. Thereafter, the lattice was accelerated with $a = 9.81 \text{ m s}^{-1}$ by ramping the frequency difference $\Delta\nu_L$ between the laser beams forming the optical lattice. After a time the lattice was switched off and the condensate was observed after an additional time-of-flight. Fig. 4(a) and (c) shows the results of these measurements in the laboratory frame. The Bloch oscillations are more evident, however, if one calculates the mean velocity v_m of the condensate as the weighted sum over the momentum components after the interaction with the accelerated lattice, as shown in Fig. 4(b). When the instantaneous lattice velocity v_{lat} is subtracted from v_m , one clearly sees the oscillatory behaviour of $v_m - v_{\text{lat}}$. The added feature of using a Bose-Einstein condensate is that the spatial extent of the atomic cloud is sufficiently small so that after a relatively short time-of-flight the separation between the individual momentum classes is already much larger than the size of the condensate due to its expansion and can, therefore, be easily resolved. Similar observations were reported in [22, 23]. In ref. [24] by using an optical Bessel beam to form the optical lattice, a very large number of Bloch oscillations of a rubidium condensate was realized and large final velocities were reached.

VI. LANDAU-ZENER TUNNELING

The linear regime of the LZ tunneling in atomic physics was investigated by several authors, using Rydberg atoms in [25], in classical optical systems in [26], for cold atoms in an accelerated optical potential in [27]. We investigated linear and nonlinear LZ tunneling between the two lowest energy bands of a condensate inside an optical lattice in the following way. Initially, the condensate was loaded adiabatically into one of the two bands. Subsequently, the lattice was accelerated in such a way that the condensate crossed the edge of the Brillouin zone once, resulting in a finite probability for tunneling into the other band (higher-lying bands can be safely neglected as their energy separation is much larger than the band gap). Thus, the two bands had populations reflecting the LZ tunneling probability (assuming only one band exclusively populated initially). In order to experimentally determine the number of atoms in the two bands, we then *increased* the lattice depth and *decreased* the acceleration. Using this experimental sequence

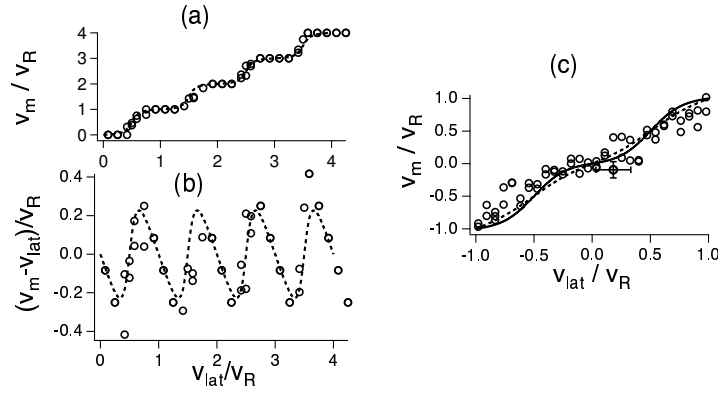


FIG. 4: Bloch oscillations of a Bose-Einstein condensate in an optical lattice. (a) Acceleration in the counterpropagating lattice with $d_L = 390 \text{ nm}$, $V_0 \approx 2.3 E_R$ and $a = 9.81 \text{ m s}^{-2}$. Dashed line: theory. (b) Bloch oscillations in the rest frame of the lattice, along with the theoretical prediction (dashed line) derived from the shape of the lowest Bloch band. (c) Acceleration in a lattice with $d_L = 1.56 \mu\text{m}$ and $V_0 \approx 11 E_R$. In this case, the Bloch oscillations are much less pronounced. Dashed and solid lines: theory for $V_0 = 11 E_R$ and $V_{eff} \approx 7 E_R$

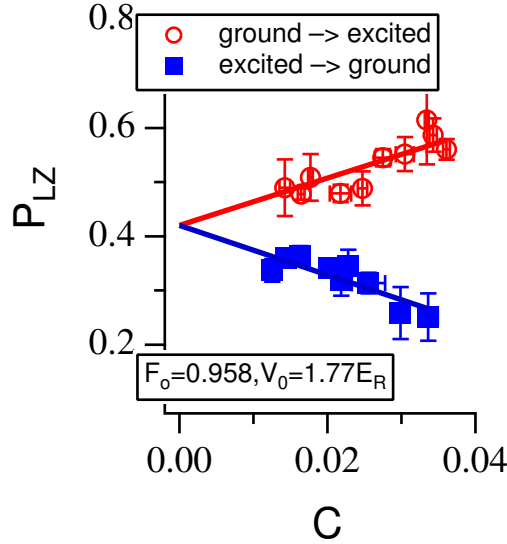


FIG. 5: Asymmetric tunneling between the ground state and first excited band of a BEC in an optical lattice as a function of the nonlinear interaction parameter C . In these experiments, $a = 32.1 \text{ m s}^{-2}$ and the lattice depth was $1.77 E_R$

we selectively accelerated further that part of the condensate that populated the ground state band, whereas the population of the first excited band was not accelerated further, as shown schematically in Fig. 2.

In order to investigate tunneling from the ground state band to the first excited band, we adiabatically ramped up the lattice depth with the lattice at rest and then started the acceleration sequence. The tunneling from the first excited to the ground-state band was investigated in a similar way, except that in this case we initially prepared the condensate in the first excited band by moving the lattice with a velocity of $1.5 v_R$ (through the frequency difference $\Delta \nu_L$ between the acousto-optic modulators) when switching it on. In this way, in order to conserve energy and momentum the condensate must populate the first excited band at a quasi-momentum half-way between zero and the edge of the first Brillouin zone. For both tunneling directions, the tunneling probability is derived from $P_{LZ} = N_{\text{tunnel}} / N_{\text{tot}}$, where N_{tot} is the total number of atoms measured from the absorption picture. For the tunneling from the first excited band to the ground band, N_{tunnel} is the number of atoms accelerated by the lattice, whereas for the inverse tunneling direction, N_{tunnel} is the number of atoms detected in the $v = 0$ velocity class.

For a small value of the interaction parameter C , we verified that the tunneling rates in the two directions are essentially the same and agree well with the linear LZ prediction. By contrast, when C is increased, the two tunneling

rates differ greatly, as in Fig. 5. We have not yet performed a quantitative comparison of these data with the theoretical predictions of the non-linear LZ model. Previous data published in [28] presented good agreement with the theoretical predictions of the asymmetric nonlinear LZ tunneling.

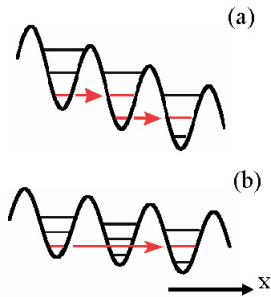


FIG. 6: The tunneling of atoms out of a tilted lattice is resonantly enhanced when the tilt induced energy difference $Fd_L\Delta i$ between lattice wells i and $i + \Delta i$ matches the separation between two quantized energy levels within a well, $\Delta i = 1$ in the top and $\Delta i = 2$ in the bottom

VII. RESONANTLY ENHANCED QUANTUM TUNNELLING

Resonantly enhanced tunneling (RET) is a quantum effect in which the probability for tunneling of a particle between two potential wells is increased when the quantized energies of the initial and final states of the process coincide. In spite of the fundamental nature of this effect and the practical interest, it has been difficult to observe experimentally in solid state structures. Quantum tunnelling has found many technological applications, for instance, in scanning tunnelling microscopes and in superconducting squid devices. The most widely application is in tunnelling diodes and related integrated semiconductor devices which go back to the pioneering work of Leo Esaki [29]. The latter also proposed to exploit resonantly enhanced tunnelling (RET) for technical use, and since the 1970's much progress has been made in producing artificial superlattice structures, in which RET of fermionic quasiparticles could be demonstrated.

Here we present our realization of RET using Bose-Einstein condensates held in optically induced potentials. The counter-propagating beams creating the lattice were continuously accelerated such as to mimic a static linear potential in the moving frame of reference. BEC tunneling occurred between the quantised energy levels (the Wannier-Stark levels) in various wells of the potential, see Fig. 6. We demonstrated that the tunneling probability is resonantly enhanced and the LZ formula does not give the correct result.

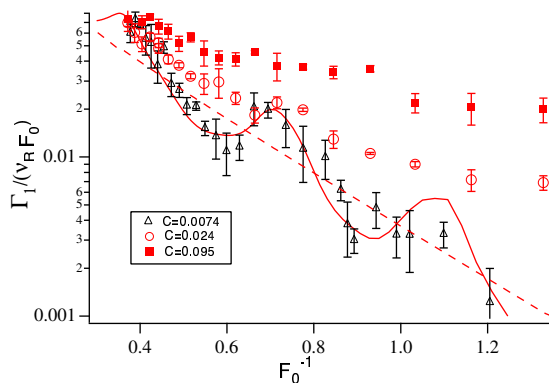


FIG. 7: Tunneling resonances of the $n = 1$ lowest energy level for $V_0 = 3.5 E_R$. The continuous line represents the theoretical RET prediction in the linear regime, and the dashed line the LZ prediction. For the experimental data (at $d_L = 426.1$ nm and $C = 0.007$) and theoretical prediction in the RET linear regime, the $\Delta i = 2$ and $\Delta i = 3$ resonant peaks appear at increasing values of F_0^{-1} , while the $\Delta i = 1$ peak is not completely scanned. In the nonlinear regimes ($d_L = 626.4$ nm, $C = 0.024$ and $d_L = 626.4$ nm, $C = 0.095$) the resonant peaks are washed out

When under the applied external force the quasimomentum explores the Brillouin zone, adiabatic transitions occur at the points of avoided crossings between the adjacent Bloch bands, for example, between the first and second bands in Fig. 2. The probability of this transition is given by the LZ tunneling formula of 11. In a first approximation, one can assume that the adiabatic transition occurs once for each Bloch cycle with the period T_B of 10. Then the population of the initial band decreases exponentially with a rate which, for the tunneling out of the ground $n = 1$ band, is given by [30]

$$\Gamma_1 = \nu_R F_0 e^{-\frac{\pi^2 V_0^2}{32 F_0}} \quad (18)$$

A plot of this tunneling rate as a function of F_0 in the linear regime is shown in Fig. 7. This regime is reached either by choosing small radial dipole trap frequencies or by releasing the BEC from the trap before the acceleration phase and thus letting it expand. In both cases, the density and hence the interaction energy of the BEC is reduced. Superimposed on the overall exponential decay of Γ_1/F_0 with F_0 , one clearly sees the resonant tunneling peaks corresponding to $\Delta i = 3, 2$. For this choice of parameters, the $\Delta i = 1$ peak lay outside the region of F values explored in the experiment. In order to highlight the deviation from the LZ prediction, the dashed line represents the prediction of 11. The experimental results are in good agreement with numerical solutions obtained by diagonalizing the Hamiltonian of the open decaying system represented by the continuous line.

Resonances in quantum tunneling for atomic motion within an optical lattice were previously observed by few authors. Evidence of RET is apparent in the Γ measurements on cold atoms of [27]. In a gray optical lattice they appear as a magnetization modulation [31]. In the demonstration of the Mott insulator phase of [5, 32] with each lattice site of Fig. 6 occupied by a single atom, RET occurred when the energy difference between neighbouring lattice sites was equal to the on-site atomic interaction energy.

VIII. CONCLUSIONS

In recent years quantum-wave transport phenomena linked to Bloch oscillations and LZ tunneling in a variety of optical lattice configurations have been widely investigated. In addition, Bloch oscillations of ultracold atoms were proposed as a tool for precision measurements of tiny forces with a spatial resolution at the micron level [33]. In [34] Bloch oscillations of ultracold atoms were performed within a few microns from a test mass in order to measure gravity with very large accuracy in order to test deviations from Newtonian law. Measurements of the recoil velocity of rubidium atoms based on Bloch oscillations lead to an accurate determination of the fine structure constant [35]. Bloch oscillations of ultracold fermionic atoms have also been proposed as a sensitive measurement of forces at the micrometer length scale, in order to perform a local and direct measurement of the Casimir-Polder force [36]. The use of quantum resonant tunneling that presents a resonant dependence on the external force may improve the accuracy of those measurements.

IX. ACKNOWLEDGMENTS

The research work presented here relied on the collaborative effort of M. Anderlini, M. Cristiani, M. Jona-Lasinio, H. Lignier, J.H. Müller, R. Mannella, C. Sias, Y. Singh, S. Wimberger and A. Zenesini. This work was supported by the European Community OLAQUI and EMALI Projects, and by MIUR-PRIN Projects.

-
- [1] O. Morsch, E. Arimondo, in *Dynamics and Thermodynamics of Systems with Long-Range Interactions*, ed. by T. Dauxois, S. Ruffo, E. Arimondo, M. Wilkens (Springer-Verlag, 2002), p. 312
 - [2] I. Bloch, J. Phys. B: At. Mol. Opt. Phys. **38**, S629 (2005)
 - [3] I. Bloch, Nat. Phys. **1**, 23 (2005)
 - [4] O. Morsch, M. Oberthaler, Rev. Mod. Phys. **78**, 180 (2006)
 - [5] M. Greiner, O. Mandel, T. Esslinger, T.W. Hänsch, I. Bloch, Nature **415**, 39 (2002)
 - [6] N. Ashcroft, N.D. Mermin, *Solid State Physics* (International Thomson Publishing, New York, 1976)
 - [7] F. Bloch, Z. Phys. **52**(7-8), 555 (1929)
 - [8] L. Landau, Phys. Z. Sowjetunion **2**, 46 (1932)
 - [9] G. Zener, Proc. R. Soc. London, Ser. A **137**, 696 (1932)
 - [10] B. Wu, Q. Niu, New J. Phys. **5**, 104 (2003)
 - [11] M.B. Dahan, E. Peik, J. Reichel, Y. Y. Castin, C. Salomon, Phys. Rev. Lett. **76**(24), 4508 (1996)

- [12] E. Peik, M. Ben Dahan, I. Bouchoule, Y. Castin, C. Salomon, Phys. Rev. A **55**(4), 2989 (1997)
- [13] E. Peik, M. Ben Dahan, I. Bouchoule, C. Salomon, Appl. Phys. B **65**, 685 (1997)
- [14] C. Waschke, H.G. Roskos, R. Schwedler, K. Leo, H. Kurz, K. Köhler, Phys. Rev. Lett. **70**(21), 3319 (1993)
- [15] V.G. Lyssenko, G. Valušis, F. Löser, T. Hasche, K. Leo, M.M. Dignam, K. Köhler, Phys. Rev. Lett. **79**(2), 301 (1997)
- [16] T. Pertsch, P. Dannberg, W. Elfle, A. Bräuer, F. Lederer, Phys. Rev. Lett. **83**(23), 4752 (1999)
- [17] R. Morandotti, U. Peschel, J.S. Aitchison, H.S. Eisenberg, Y. Silberberg, Phys. Rev. Lett. **83**(23), 4756 (1999)
- [18] H. Trompeter, W. Krolikowski, D.N. Neshev, A.S. Desyatnikov, A.A. Sukhorukov, Y.S. Kivshar, T. Pertsch, U. Peschel, F. Lederer, Phys. Rev. Lett. **96**(5), 053903 (2006)
- [19] H. Sanchis-Alepuz, Y.A. Kosevich, J. Sánchez-Dehesa, Phys. Rev. Lett. **98**(13), 134301 (2007)
- [20] O. Morsch, J.H. Müller, M. Cristiani, D. Ciampini, E. Arimondo, Phys. Rev. Lett. **87**(14), 140402 (2001)
- [21] M. Cristiani, O. Morsch, J.H. Müller, D. Ciampini, E. Arimondo, Phys. Rev. A **65**(6), 063612 (2002)
- [22] J. Hecker Denschlag, J. Simsarian, H. Häffner, C. McKenzie, A. Browaeys, D. Cho, K. Helmerson, S. Rolston, W.D. Phillips, J. Phys. B: At. Mol. Opt. Phys. **35**(14), 3095 (2002)
- [23] A. Browaeys, H. Häffner, C. McKenzie, S.L. Rolston, K. Helmerson, W.D. Phillips, Phys. Rev. A **72**(5), 053605 (2005)
- [24] S. Schmid, G. Thalhammer, K. Winkler, F. Lang, J.H. Denschlag, New J. Phys. **8**(8), 159 (2006)
- [25] J.R. Rubbmark, M.M. Kash, M.G. Littman, D. Kleppner, Phys. Rev. A **23**(6), 3107 (1981)
- [26] D. Bouwmeester, N.H. Dekker, F.E.v. Dorsselaer, C.A. Schrama, P.M. Visser, J.P. Woerdman, Phys. Rev. A **51**(1), 646 (1995)
- [27] C.F. Bharucha, K.W. Madison, P.R. Morrow, S.R. Wilkinson, B. Sundaram, M.G. Raizen, Phys. Rev. A **55**(2), R857 (1997)
- [28] M. Jona-Lasinio, O. Morsch, M. Cristiani, N. Malossi, J.H. Müller, E. Courtade, M. Anderlini, E. Arimondo, Phys. Rev. Lett. **91**(23), 230406 (2003). Erratum *ibidem* **93**(11), 119903 (2004)
- [29] L. Esaki, in *Nobel Lectures, Physics 1971-1980*, ed. by S. Lundqvist (World Scientific, Singapore, 1992)
- [30] Q. Niu, X.G. Zhao, G.A. Georgakis, M.G. Raizen, Phys. Rev. Lett. **76**(24), 4504 (1996)
- [31] B.K. Teo, J.R. Guest, G. Raithel, Phys. Rev. Lett. **88**(17), 173001 (2002)
- [32] M. Greiner, Ultracold quantum gases in three-dimensional optical lattice potentials. Ph.D. thesis, Ludwig-Maximilians-Universität München (2003)
- [33] P. Cladé, S. Guellati-Khélifa, C. Schwob, F. Nez, L. Julien, F. Biraben, Europhys. Lett. **71**(5), 730 (2005)
- [34] G. Ferrari, N. Poli, F. Sorrentino, G.M. Tino, Phys. Rev. Lett. **97**(6), 060402 (2006)
- [35] P. Cladé, E. de Mirandes, M. Cadoret, S. Guellati-Khélifa, C. Schwob, F. Nez, L. Julien, F. Biraben, Phys. Rev. Lett. **96**(3), 033001 (2006)
- [36] I. Carusotto, L. Pitaevskii, S. Stringari, G. Modugno, M. Inguscio, Phys. Rev. Lett. **95**(9), 093202 (2005)